THE JOURNAL OF BIOLOGICAL CHEMISTRY VOL. 289, NO. 6, pp. 3198–3208, January 7, 2014

Three Different Classes of Aminotransferases Evolved Prephenate Aminotransferase Functionality in Arogenate-competent Microorganisms*

Received for publication, May 17, 2013, and in revised form, November 8, 2013 Published, JBC Papers in Press, December 3, 2013, DOI 10.1074/jbc.M113.486480

Matthieu Graindorge[‡§1], Cécile Giustini[‡¶], Alexandra Kraut[‖], Lucas Moyet[‡2], Gilles Curien[‡**3], and Michel Matringe[‡¶4]**

*From the [‡]Commissariat à l'Energie Atomique, Direction des Sciences du Vivant, institut de Recherches en Technologies et en Sciences pour le Vivant, Laboratoire de Physiologie Cellulaire et Végétale, F-38054 Grenoble, France, [§]Université Grenoble Alpes, F-38054 Grenoble, France, [¶]Institut National de la Recherche Agronomique, USC1359, F-38054 Grenoble, France, [‖]INSERM, Laboratoire d'Etude de Dynamique des Protéomes, U880, F-38054 Grenoble, France, and **CNRS, UMR 5168, 17 Rue des Martyrs, F-38054 Grenoble, France*

Background: The genes encoding prephenate aminotransferase in arogenate-competent microorganisms for tyrosine synthesis are still unknown.
Results: Three different classes of aminotransferase use prephenate as an amino acceptor.
Conclusion: Prephenate aminotransferase functionality has arisen more than once during evolution.
Significance: This first identification of prephenate aminotransferases in arogenate competent microorganisms affords a better understanding of the origin and fixation of the arogenate route during evolution.

The aromatic amino acids phenylalanine and tyrosine represent essential sources of high value natural aromatic compounds for human health and industry. Depending on the organism, alternative routes exist for their synthesis. Phenylalanine and tyrosine are synthesized either via phenylpyruvate/4-hydroxyphenylpyruvate or via arogenate. In arogenate-competent microorganisms, an aminotransferase is required for the transamination of prephenate into arogenate, but the identity of the genes is still unknown. We present here the first identification of prephenate aminotransferases (PATs) in seven arogenate-competent microorganisms and the discovery that PAT activity is provided by three different classes of aminotransferase, which belong to two different fold types of pyridoxal phosphate enzymes: an aspartate aminotransferase subgroup 1β in tested α- and β-proteobacteria, a branched-chain aminotransferase in tested cyanobacteria, and an *N*-succinyldiaminopimelate aminotransferase in tested actinobacteria and in the β-proteobacterium *Nitrosomonas europaea*. Recombinant PAT enzymes exhibit high activity toward prephenate, indicating that the corresponding genes encode *bona fide* PAT. PAT functionality was acquired without other modification of substrate specificity and is not a general catalytic property of the three classes of aminotransferases.

The aromatic amino acid biosynthesis pathway is only found in microorganisms and plants and never occurs in animals. This pathway links the metabolism of carbohydrates to the biosynthesis of aromatic amino acids involved in protein synthesis and the metabolism of a large diversity of aromatic secondary metabolites (1–3). The aromatic amino acid biosynthesis pathway is thus of central importance for the growth of these organisms and for their interaction with their environment. Phenylalanine and tyrosine also represent an important source of high value aromatic natural compounds for industry and for human health.

Two alternative routes for the post-chorismate branch of the pathway leading to tyrosine exist: the 4-hydroxyphenylpyruvate route or the arogenate route (Fig. 1). For the majority of green bacteria and many other microorganisms, L-tyrosine is synthesized via the arogenate route (4–6). Prephenate, in this case, is transaminated into arogenate by a specific transaminase before being decarboxylated into L-tyrosine by an arogenate dehydrogenase (EC 1.3.1.43). Alternatively, in microorganisms, such as *Escherichia coli*, prephenate is first transformed into 4-hydroxyphenylpyruvate by a prephenate dehydrogenase (EC 1.3.1.13) and then transaminated into L-tyrosine (7). In other microorganisms, such as *Zymomonas mobilis* and *Pseudomonas aeruginosa*, a single enzyme termed cyclohexadienyl dehydrogenase can use either arogenate or prephenate as a substrate (8, 9). Most organisms use the arogenate route exclusively for tyrosine biosynthesis; however, the vast majority of plants are the sole documented organisms that synthesize both tyrosine and phenylalanine via the arogenate route (10–17). Prephenate

* This work was supported in part by the French National Institute for Agricultural Research (INRA), CNRS, and the Commissariat à l'Energie Atomique et aux Energies Alternatives (CEA).

The amino acid sequences of the proteins characterized in this study can be accessed through the UniProt database under the following UniProt accession numbers: Q02635, A3PMF8, P54691, Q55128, Q55828, Q3AJX2, Q82IK5, Q82DR2, Q82JN7, Q82EU6, O50434, Q82WA8, Q82UJ8, Q82S89, and Q82TJ4.

[1] Supported by a Ph.D. fellowship from the University of Grenoble Alpes.
[2] Supported by a grant from the GRAL Labex (Grenoble Alliance for Integrated Structural Cell Biology: ANR-10-LABEX-04).

[3] To whom correspondence may be addressed: Laboratoire de Physiologie Cellulaire et Végétale, CEA iRTSV, CNRS, UMR 5168, 17 Rue des Martyrs, Grenoble 38054, France. Tel.: 33-4-38-782-364; Fax: 33-4-38-785-091; E-mail: gilles.curien@cea.fr.
[4] To whom correspondence may be addressed: Laboratoire de Physiologie Cellulaire et Végétale, CEA iRTSV, CNRS, UMR 5168, 17 Rue des Martyrs, Grenoble 38054, France. Tel.: 33-4-38-782-364; Fax: 33-4-38-785-091; E-mail: michel.matringe@cea.fr.

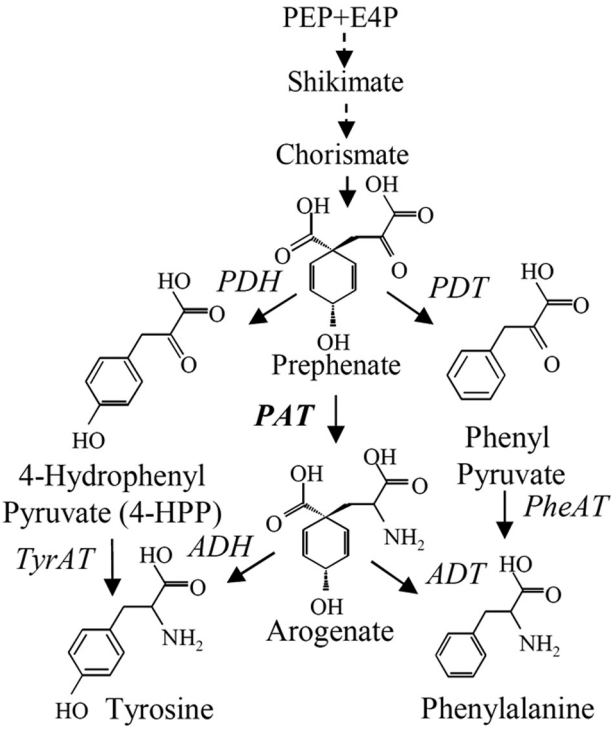

FIGURE 1. **Tyrosine and phenylalanine biosynthesis pathways.** The two alternatives for the synthesis of tyrosine and phenylalanine are represented. Multiple enzymatic steps involved are shown by *dotted lines*. *ADH*, arogenate dehydrogenase; *ADT*, arogenate dehydratase; *E4P*, erythrose 4-phosphate; *PDH*, prephenate dehydrogenase; *PDT*, prephenate dehydratase; *PEP*, phosphoenolpyruvate; *Phe-AT*, phenylalanine aminotransferase; *TYR-AT*, tyrosine aminotransferase.

aminotransferase (PAT)[5] activity has only recently been identified in plants (18, 19). PAT activity in *Arabidopsis thaliana* is carried out by an aspartate aminotransferase (AAT/PAT, *At2g22250* gene; EC 2.6.1.1, EC 2.6.1.78, and EC 2.6.1.79) (18, 19). This aminotransferase belongs to subgroup 1β (20) of the aspartate aminotransferases (1β AAT). In a previous study, we showed that this enzyme is bispecific, catalyzing the transamination of oxaloacetate into aspartate as efficiently as prephenate into arogenate (18). In microorganisms, PAT activity was previously detected in cyanobacteria, actinobacteria, and some proteobacteria (4, 6, 21). However, the genes coding the aminotransferases responsible for PAT activity in these microorganisms remain to be identified.

In the present work, biochemical analyses and mass spectrometry identification were combined to identify the genes responsible for arogenate synthesis in arogenate-competent microorganisms (cyanobacteria, α- and β-proteobacteria, and actinobacteria). It appeared that *bona fide* PAT activity can be hosted by three different aminotransferases, which belong to two different fold types of pyridoxal phosphate (PLP)-dependent enzymes. The capacity to transaminate prephenate was acquired without other modification of substrate property and is not a general catalytic property of the three classes of aminotransferases. The evolutionary implications of these results are discussed.

EXPERIMENTAL PROCEDURES

Culture of Bacteria—Rhizobium meliloti RCR2011 strain was kindly provided by G. Alloing (UMR 6192, Sophia Antipolis, France) and grown at 30 °C in LB medium supplemented with 2.5 mM $MgSO_4$, 2.5 mM $CaCl_2$, and 200 $\mu g \cdot ml^{-1}$ streptomycin sulfate. *Synechocystis* sp. PCC 6803 strain was kindly provided by G. Ajlani (UMR 8221, Saclay, France) and grown at 30 °C under constant light (200 microeinsteins) in BG11 medium. The *Streptomyces avermitilis* strain was kindly provided by P. Mazolier (Institut Pasteur, Paris, France), and grown at 30 °C in LB medium supplemented with 0.5% starch with glass beads to avoid the formation of bacterial aggregates. The *Rhodobacter sphaeroides* strain was kindly provided by M. Sabaty (UMR6191, CEA, Cadarache, France) and grown in Sistrom medium at 30 °C. Genomic DNA of *Nitrosomonas europea* (ATCC 19718) was kindly provided by B. Cherif-Zahar (INSERM U845, Paris, France). Genomic DNA of *Synechococcus* CC9605 was kindly provided by F. Partensky (UMR 7144, Roscoff, France). Genomic DNA of *Mycobacterium tuberculosis* (strain H37rv) was kindly provided by B. Gicquel (UMR 5092, Toulouse, France).

Preparation of Crude Extracts and Protein Purification—Cells were harvested by centrifugation (4000 × *g*, 45 min), and pellets were resuspended in 30 ml of 25 mM Hepes, pH 8.0, 1 mM EDTA, 1 mM DTT, 10% glycerol (v/v), 50 μM PLP, 5 mM ϵ-aminocaproic acid, and 1 mM benzamidine and sonicated for 10 min at 4 °C on a Branson sonicator. Streptomycin sulfate (0.1% (w/v)) was added to precipitate DNA, and the extract was centrifuged for 45 min at 40,000 × *g* (Sorvall SS-34) at 4 °C. Purifications were carried out at room temperature. Crude extract was loaded onto 130 ml of EMD DEAE 650(M) resin (Merck) in an XK 26 column (26 × 260 mm^2, Amersham Biosciences) equilibrated with buffer A: 25 mM Hepes, pH 8.0, 1 mM EDTA, 1 mM DTT, 10% glycerol (v/v), 50 μM PLP. Proteins were eluted with a linear gradient of NaCl in this buffer. Active fractions were pooled and desalted and loaded onto 10 ml of Q-Sepharose resin (GE Healthcare) in a XK-16 column (Amersham Biosciences), equilibrated with buffer A. Proteins were eluted by a linear gradient (0–0.5 M) of NaCl in buffer A. Active fractions were pooled and loaded onto HiPrep 16/60 Sephacryl S-200 column (Amersham Biosciences) equilibrated with buffer A supplemented with 100 mM NaCl. Active fractions were pooled and desalted and loaded onto a MonoQ column (UnoQ1, Bio-Rad) equilibrated with buffer A. Proteins were eluted with a linear gradient of NaCl in this buffer. Active fractions were concentrated using a 500-μl Amicon® ultrafiltration unit, frozen in liquid nitrogen, and stored at −80 °C.

Identification of Prephenate Aminotransferases—The elution profile of PAT activity and SDS-PAGE analyses of the active fractions eluted from the last MonoQ column were compared. A unique polypeptide band co-eluting with PAT activity was identified, and the corresponding gel band in the most active fraction was cut from the gel (see Fig. 3 as an example). The

[5] The abbreviations used are: PAT, prephenate aminotransferase; 1,2-HGAD, 1,2-homogentisate dioxygenase; 4-HPP, 4-hydroxyphenylpyruvate; 4-HPPD, 4-hydroxyphenylpyruvate dioxygenase; AAT, aspartate aminotransferase; BCAT, branched-chain aminotransferase; S-DAP, *N*-succinyl-LL-diaminopimelate; DAPAT, diaminopimelate aminotransferase; S-DAPAT, succinyldiaminopimelate aminotransferase; PLP, pyridoxal phosphate.

TABLE 1
Primers used for cloning the different aminotransferases

Primers	Sequences
Primer 5′	
Rme_Q02635	CAGGAAACACCATATGGCCTTCCTTGC
Rsp_A3PMF8	GAGTTTCCCCCATATGGCCTTCCTCTC
Syn_P54691	TTTTTTGATTTTCATATGCACAAGTTTTT
Syn_Q55128	GGGATGTTTTGCATATGCGACTAACCCAGC
Syn_Q55828	gatcgccctttaatcaccaacatatggccagtatcaacg
Sco_Q3AJX2	CGGATCCATCACTCATATGCATCAGTTCCTGCCCTATGCCTGG
Sav_Q82IK5	GTGAGTCCGATCCATATGTCCGCAGTCTCCGA
Sav_Q82DR2	GATGGGTCATATGAGCGCTGC
Sav_Q82JN7	GGTGAAGGACAACCACATATGACGACGCCCACGAT
Sav_Q82EU6	CCAGAGCTTCGGCGCCATATGGCGGCCATGA
Mtu_O50434	gctcgcggccatatgtcggcgtctctgcccgtcttcc
Neu_Q82WA8	ATCAGGAGCTGTCATATGAACCTCTCGCAACG
Neu_Q82UJ8	GCAGACAATAAAAACACATATGATTTACCTCAAT
Neu_Q82S89	CAATCTTGAGAACATATGAATCCTTCACTGGAA
Neu_Q82TJ4	CACAGGAGAGTTTCCATATGTCGATGGCGGACCGTGA
Primer 3′	
Rme_Q02635	CATGTCGGTCTGCTCGAGAATTATCTGC
Rsp_A3PMF8	ATCCTGCTCATGGAGCTCTTCTGGCTCC
Syn_P54691	ATCTTGCCAGGAGCTCTTAGCCATTCAAAGG
Syn_Q55128	GGGTTGGACGGGAGCTCAAGCCAAAGTGC
Syn_Q55828	ctagagctacctttgggagctcttctaacccaatttgagg
Sco_Q3AJX2	CTTCAGCCGTTGAGCTCAGGCAATGGAAATGCGGGTCACCCAGTGC
Sav_Q82IK5	CGCCTGGCGTAGCGAGCTCGCACACGGCGACG
Sav_Q82DR2	GGCGTACGAAGAGCTCAGTCCTTCGC
Sav_Q82JN7	GAGGGCGAGGCCCTCTCGAGCTAGCCCAGCGGGT
Sav_Q82EU6	CGGCCTCGCGGCCTCGAGTCAGCCGCGCAGCGT
Mtu_O50434	cgcaagttgcgaagcttcgcgctaacaggtgagccg
Neu_Q82WA8	CGTCATCAAAAAGTGTCGAGAGCTCAGCTCAGTAAAC
Neu_Q82UJ8	ACGTTTTTCAGAGCTCCCTTAGAGCAGCATGGTT
Neu_Q82S89	CCTAAAAAAATAATGAGCTCAGAATTTTCT
Neu_Q82TJ4	GTTCAACAGTTAAACATAAGAGCTCTAATCGGCGTAA

peptides contained in this gel band were prepared for LC-MS analyses as described (22). Nanoliquid chromatography LTQ-Orbitrap and bioinformatic analyses were performed as described (23).

Determination of Enzyme Activities—Glutamate-oxaloacetate aminotransferase and aspartate-α-ketoglutarate aminotransferase activities were assayed as described (18). Branched-chain aminotransferase (BCAT) activity was assayed by coupling the reaction with glutamate dehydrogenase. Reaction mix contained 50 mM Hepes, pH 8.0, 50 mM NH_4Cl, 25 mM glutamate, 200 μM NADH, 6 units of glutamate dehydrogenase, and variable concentrations of the keto acid 4-methyl-2-oxovalerate, 3-methyl-2-oxovalerate, or 3-methyl-2-oxobutyrate. Activity was measured by monitoring oxidation of NADH at 340 nm. For *N*-succinyldiaminopimelate aminotransferase activity, *N*-succinyldiaminopimelate was kindly provided by Dr. Mengin-Lecreulx, and the enzyme activity was assayed by following the *N*-succinyldiaminopimelate-dependent formation of glutamate from α-ketoglutarate. A 10-μl aliquot of reaction medium was derivatized for 1 min with *o*-phtaldialdehyde prior to its injection onto a Spherisorb ODS2 C18 column connected to an Agilent 1100 HPLC system. Elution was carried out at 1 ml/min with a 10–60% methanol gradient (15 min) in 50 mM potassium phosphate buffer (pH 6.9). The *o*-phtaldialdehyde derivatives of amino acids were detected by fluorescence (excitation, 360 nm; emission, 455 nm). Glutamate was identified by comparison with an authentic standard. For the analyses of the substrate specificity of the different PATs, the capacity to transfer the amino group of glutamate to different keto acids was monitored by coupling the reaction with glutamate dehydrogenase as described for BCAT activity measurement (see above). Prephenate aminotransferase activities were assayed by coupling the reaction with purified Tyr-insensitive arogenate-specific dehydrogenase from *Synechocystis* (24) and following the reduction of NADP at 340 nm. The reaction was carried out at 30 °C in 50 mM Hepes buffer (pH 8.0) in the presence of 40 nM coupling enzyme, 100 μM NADP, and variable amounts of prephenate, aspartate, glutamate, leucine, isoleucine, or *N*-succinyl-LL-diaminopimelate (S-DAP). Activities were calculated using an ϵ for NADPH of 6250 $M^{-1}\cdot cm^{-1}$ at 340 nm. Arogenate formation was confirmed by HPLC analyses as described (18).

Construction of Recombinant Vectors—Primers used for amplification of the aminotransferase genes from the corresponding genomic DNA are presented in Table 1. Restriction sites introduced by PCR are underlined. These genes were cloned into pET30 b(+) vector, and the recombinant proteins were produced without any tag with the exception of Sav_Q82EU6, which was cloned into pET28 b(+) vector.

Overproduction and Purification of Recombinant Proteins—Fresh colonies of transformed BL21 (DE3) Rosetta2 bacteria (Novagen, Darmstadt, Germany) were transferred into 15 ml of LB medium supplemented with the appropriate antibiotics and grown at 37 °C. Saturated culture was transferred into 800 ml of LB medium supplemented with the antibiotics, and growth was continued until $A_{600\ nm} = 0.6$. IPTG (0.4 mM) was added to the medium, and the bacteria were grown at 20 °C for 16 h. The crude extract was prepared as described for the native proteins. Purification of recombinant proteins was performed as follows. Crude extract of soluble proteins (20–50 mg) was loaded on 10 ml of Q-Sepharose resin (GE Healthcare) in an XK-16 column (Amersham Biosciences), equilibrated with Buffer A. Proteins

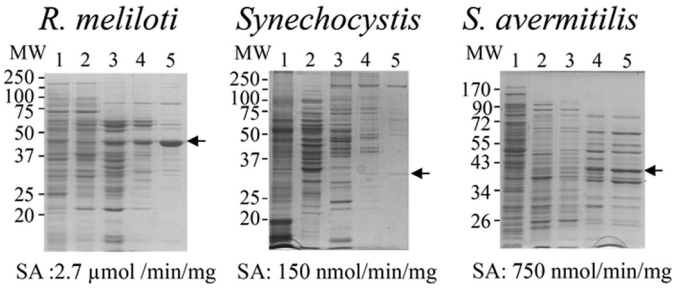

FIGURE 2. **Purification of native PAT from crude extracts of soluble proteins from *R. meliloti*, *Synechocystis*, and *S. avermitilis*.** Proteins were separated on SDS-polyacrylamide gels (12% acrylamide) and stained with Coomassie Brilliant Blue R-250. *Lane 1*, crude extract; *lane 2*, pool of active fractions eluted from the EMD DEAE 650(M) column; *lane 3*, pool of active fractions eluted from the Q-Sepharose HP column; *lane 4*, pool of active fractions eluted from the HiPrep 16/60 Sephacryl S-200 column; *lane 5*, most active fractions eluted from the MonoQ column. SDS-PAGE analyses of the active fractions eluted from the last MonoQ columns revealed for each cellular extract a unique gel band that exactly follows the PAT activity profile of these fractions (see Fig. 3 for an example). These gel bands (*arrows*) were cut from the gel in the most active fractions and submitted to MS identification. In all three cases, the major polypeptide present in the analyzed gel band, on the basis of the spectral counts observed, corresponded to an aminotransferase: an aspartate aminotransferase (Q02635) for *R. meliloti*, a branched-chain aminotransferase (P54691) for *Synechocystis*, and a succinyldiaminopimelate aminotransferase (Q82IK5) from *S. avermitilis* (see Fig. 4). *SA*, PAT-specific activity of the most active fraction eluted from the last MonoQ column.

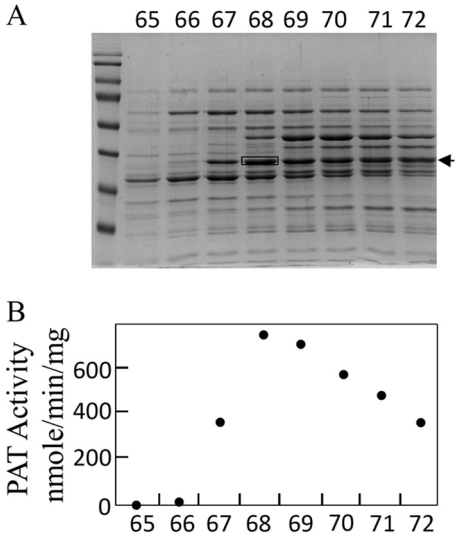

FIGURE 3. **Identification of the protein harboring PAT activity from *S. avermitilis* cellular extract.** *A*, SDS-PAGE of active fractions eluted from the last MonoQ column (UnoQ1, Bio-Rad). *B*, PAT activity profile of active fractions eluted from the MonoQ column (UnoQ1, Bio-Rad). According to this PAT activity profile, only one gel band exactly follows it (*arrow*). The peptides contained in this gel band were cut from the gel in fraction 68 (*black box*) and submitted to MS identification (see Fig. 4). A similar procedure was used for the identification of the protein harboring PAT activity from *R. meliloti* and *Synechocystis*.

were eluted by a linear gradient (0–0.5 M) of NaCl in buffer A. Active fractions were pooled and loaded on HiPrep 16/60 Sephacryl S-200 column (Amersham Biosciences) equilibrated with Buffer A supplemented with 100 mM NaCl. Active fractions were pooled, desalted in buffer A supplemented with 10% glycerol, frozen in liquid nitrogen, and stored at −80 °C. Recombinant Sav_Q82EU6 was purified by a nickel-nitrilotriacetic acid affinity column.

R. meliloti: 1β AAT Q02635

Accession	Description	score	Mass	Cov.	Pep.	EmPAI	SC
Q02635	1β Aspartate aminotrans.	211.15	43555.06	68.00	25	10.52	157
Q92QU6	Serine hydroxymethyltransf.	1923.33	46702.84	68.68	23	7.07	102
Q92P61	6-phosphogluconate dehydro.	1987.86	50772.15	68.49	22	8.23	75
Q92SR3	Aminopeptidase	1417.41	45105.85	68.05	17	4.05	56
Q92PG6	Isocitrate dehydrogenase	1342.71	45145.04	56.59	16	2.86	24
Q9EYG9	Succinyl-CoA ligase	1083.07	42108.18	51.79	13	1.95	17
Q92PR7	Molybdopterin biosynthesis	909.98	42564.48	36.66	9	1.36	15
Q92LM0	ABC transporter Subunit	986.97	64004.43	30.81	13	0.95	14
Q92TH0	Uncharacterised	1004.89	45486.15	42.37	11	1.23	13
Q92T27	Glucokinase	511.67	35777.62	41.49	7	0.97	9
P58350	Aspartate aminotransferase	407.02	44346.73	17.37	6	0.62	7
Q92SC4	Glucose-6-phosphateiso.	303.34	58574.17	12.59	4	0.23	4
Q92U16	Acriflavin resistance	238.33	39240.65	9.92	2	0.17	2
Q92VF4	Pilin glycosylation	242.81	43554.16	9.87	2	0.15	2

Synechocystis: BCAT P54691

Accession	Description	score	Mass	Cov.	Pep.	EmPAI	SC
P54691	Branched Chain Aminotrans.	1885.30	33929.56	80.52	22	19.81	165
P74729	HrEpiB	243.25	34929.00	15.14	4	0.42	4
Q55517	Sii0529 protein	272.05	78267.28	7.59	4	0.17	4
P74469	Sii0135 protein	154.88	35296.17	8.44	2	0.19	2
P55038	Feredoxin-dep. gluta. Synth.	132.52	169392.2	1.82	2	0.04	2

S. Avermitilis: S-DAPAT Q82IK5

Accession	Description	score	Mass	Cov.	Pep.	EmPAI	SC
Q82IK	Apartae aminotransfer.	1005.56	39266.38	55.68	14	5.90	128
Q82DI5	60 KD chaperonin 1	934.79	56961.99	28.05	13	1.99	30
Q82GG6	60 KD chaperonin 2	793.51	56766.93	22.48	10	1.50	26
Q82FX0	Valine dehydrogenase	458.81	38030.33	32.38	9	1.47	12
Q82FF7	1L-myoino.-1-phosph. Synth.	399.21	39417.15	24.58	7	1.01	10
Q82J82	ATP synthase subunit8	440.83	57229.26	24.42	9	0.72	9
Q826P3	Dehydrogenase	196.38	36277.01	17.33	4	0.46	4
Q828N6	Idonate dehydrogenase	165.88	34807.99	13.61	3	0.48	4
Q82E21	Glut.-1-semiald.-1.2-aminomut.	97.53	45747.85	5.34	2	0.16	2
Q82JI2	Aminomethyltransferase	103.63	39063.01	6.20	2	0.19	2
Q82HR6	folDE2 protein	70.88	29648.68	13.01	2	0.26	2

FIGURE 4. **MS identification of peptides contained in the gel band following PAT activity profiling and cut from the gel (arrows in Figs. 2 and 3).** In the three cases, the most abundant peptides, on the basis of the spectral counts observed, corresponded to an aminotransferase: an aspartate aminotransferase (Q02635) for *R. meliloti*, a branched-chain aminotransferase (P54691) for *Synechocystis*, and a succinyldiaminopimelate aminotransferase (Q82IK5) for *S. avermitilis*.

RESULTS

Identification of Prephenate Aminotransferase in R. meliloti, Synechocystis, and S. avermitilis—To identify the protein carrying PAT activity in bacteria known to use the arogenate route for tyrosine biosynthesis, PAT activity was partially purified from cellular extracts of the α-proteobacterium *R. meliloti*, the cyanobacterium *Synechocystis* sp. (PCC 6803), and the actinobacterium *S. avermitilis* in a four-step process (see "Experimental Procedures" and Fig. 2). For the three cellular extracts, PAT activity eluted in a single peak at each purification step, and SDS-PAGE analyses of the active fractions eluted from the last MonoQ columns revealed for each cellular extract a unique gel band, which exactly followed the PAT activity profile of these fractions (see Fig. 3 as an example). The corresponding gel band in the most active fraction was extracted from the SDS-PAGE, and the polypeptides were analyzed by mass spectrometry and identified (22, 23). The major polypeptide present in the analyzed gel band, on the basis of the spectral counts observed, corresponded to 1β AAT (Rme_Q02635) (EC 2.6.1.1) in *R. meliloti*, to a BCAT (Syn_P54691) (EC 2.6.1.42) in *Synechocystis*, and to an *N*-succinyldiaminopimelate aminotransferase (S-DAPAT) (Sav_Q82IK5) (EC 2.6.1.17) in *S. avermitilis* (Fig. 4). The corresponding genes

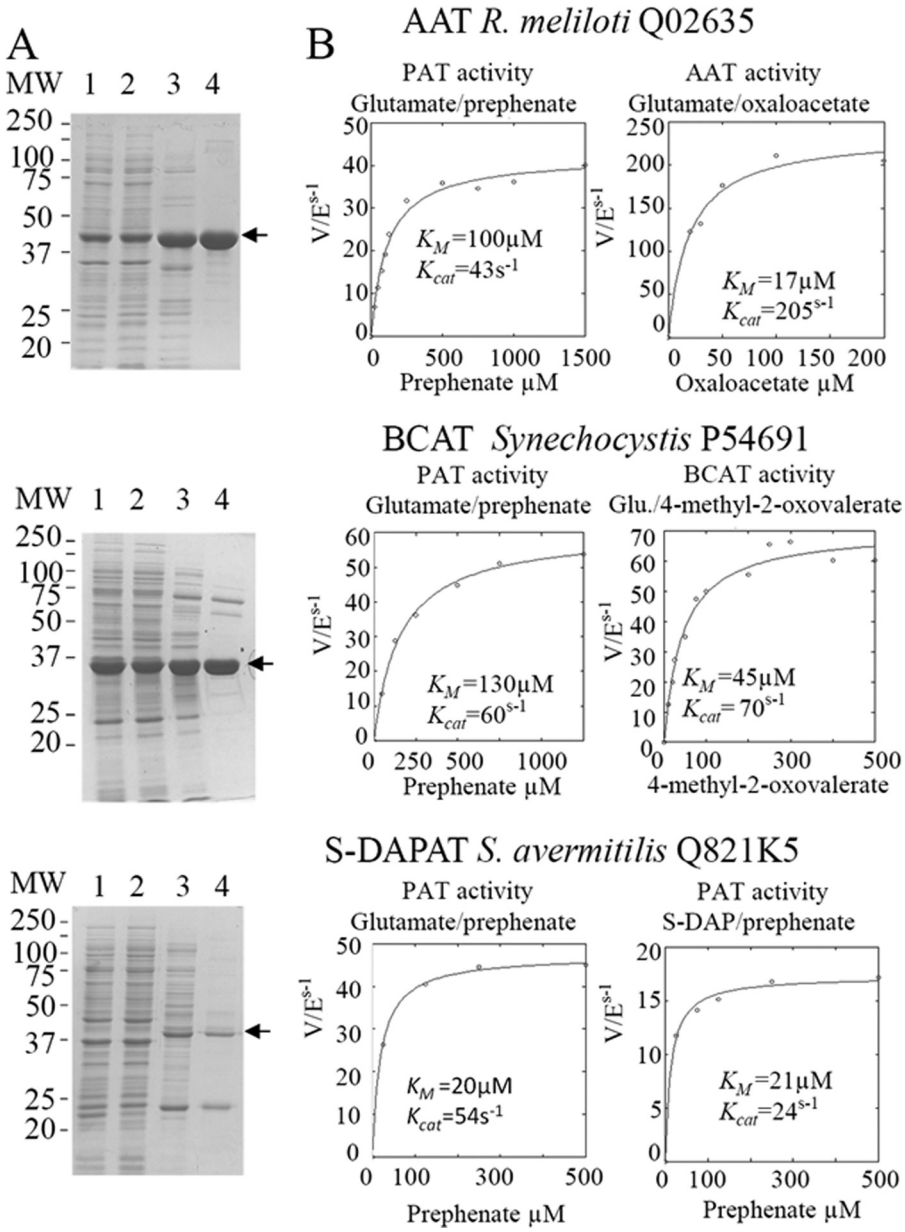

FIGURE 5. **Partial purification and kinetic analyses of the recombinant PAT enzymes.** *A*, expression and purification of recombinant PAT enzymes. Proteins were separated on SDS-polyacrylamide gels (12% acrylamide). *Lane 1*, total protein extract; *lane 2*, crude extract of soluble proteins (15 μg); *lane 3*, pool of active fractions eluted from the EMD DEAE 650(M) column (Merck); *lane 4*, pool of active fractions eluted from the HiPrep 16/60 Sephacryl S-200 column (Amersham Biosciences). *B*, kinetic analyses of the recombinant PAT enzymes. Kinetic parameters (k_{cat} and K_m) were determined for the three enzymes in the presence of their native keto acid substrate or in the presence of prephenate, with glutamate as an amino-donor.

were cloned, and the recombinant proteins were overproduced in *E. coli* and partially purified (Fig. 5*A*). Their ability to transaminate prephenate was confirmed. Detailed kinetic characterizations (Table 2 and Fig. 5*B*) were then carried out to determine the efficiency of these proteins to transaminate the keto acid prephenate with glutamate as an amino donor and to examine how this additional kinetic competence compared with the original AAT, BCAT, and S-DAPAT activities. The kinetic parameters of AAT (Rme_Q02635), BCAT (Syn_P54691), and S-DAPAT (Sav_Q82IK5) displayed in Fig. 5 and Table 2 indicate that, in the presence of glutamate as an amino donor, the three enzymes efficiently transaminate prephenate and thus can be considered *bona fide* PATs. Indeed, k_{cat} values for arogenate synthesis in the presence of glutamate were 43 s^{-1} for AAT/PAT (Rme_Q02635) and 60 s^{-1} for BCAT/PAT (Syn_P54691). These k_{cat} values are similar to the BCAT activity or slightly lower than the AAT activity. K_m values for prephenate were in the range of 20–300 μM (Fig. 5 and Table 2).

S-DAPAT is involved in the synthesis of lysine in some bacteria (25) and catalyzes the transamination of the keto acid *N*-succinyl-L-2-amino-6-oxopimelate into S-DAP (Fig. 6). We were able to obtain *N*-succinyl-LL-diaminopimelate, and this allowed us to confirm that Sav_Q82IK5, which had not been previously characterized, could indeed use S-DAP as an amino donor to transaminate prephenate (Fig. 5 and Table 2) or α-ketoglutarate (Fig. 6*B*). Its capacity to transaminate prephenate compares well with AAT/PAT and BCAT/PAT (k_{cat} = 54 s^{-1}).

TABLE 2

Kinetic parameters of recombinant prephenate aminotransferases

Values given are the average of at least three independent determinations. The difference in each set of data was <10%.

AAT/PAT	Prephenate (25 mM Glu)			Oxaloacetate (25 mM Glu)		
	K_M (μM)	k_{cat} (s^{-1})	k_{cat}/K_M	K_M (μM)	k_{cat} (s^{-1})	k_{cat}/K_M
Rme_Q02635	100	43	0.43	17	205	12
Rsp_A3PMF8	290	56	0.2	27	150	5.6
Neu_Q82WA8	400	0.8	0.002	35	33	0.9
BCAT/PAT	Prephenate (25 mM Glu)			4-MOV (25 mM Glu)		
	K_M (μM)	k_{cat} (s^{-1})	k_{cat}/K_M	K_M (μM)	k_{cat} (s^{-1})	k_{cat}/K_M
Syn_P54691	130	60	0.46	45	70	1.55
Sco_Q3AJX2	280	21	0.08	27	130	4.8
S-DAPAT/PAT	Prephenate (25 mM Glu)			Prephenate (2 mM S-DAP)		
	K_M (μM)	k_{cat} (s^{-1})	k_{cat}/K_M	K_M (μM)	k_{cat} (s^{-1})	k_{cat}/K_M
Sav_Q82IK5	20	54	2.7	13	20	1.5
Mtu_O50434	70	40[b]	0.6	ND[a]	ND[a]	-
Neu_Q82S89	160	70[b]	0.8	ND[a]	ND[a]	-

[a] The capacity of *M. tuberculosis* (Mtu_O50434) and *N. europea* (Neu_Q82S89) to catalyze the transamination of prephenate with S-DAP as amino donor was confirmed, but the kinetics parameters were not determined.

[b] k_{cat} value for *M. tuberculosis* O50434 and *N. europea* (Neu_Q82S89) S-DAPAT/PAT were corrected assuming a degree of purity of 30 and 10%, respectively (see Figs. 8 and 9). No activity could be detected in the corresponding non-induced crude extracts. 4-MOV, 4-methyl-2-oxovalerate.

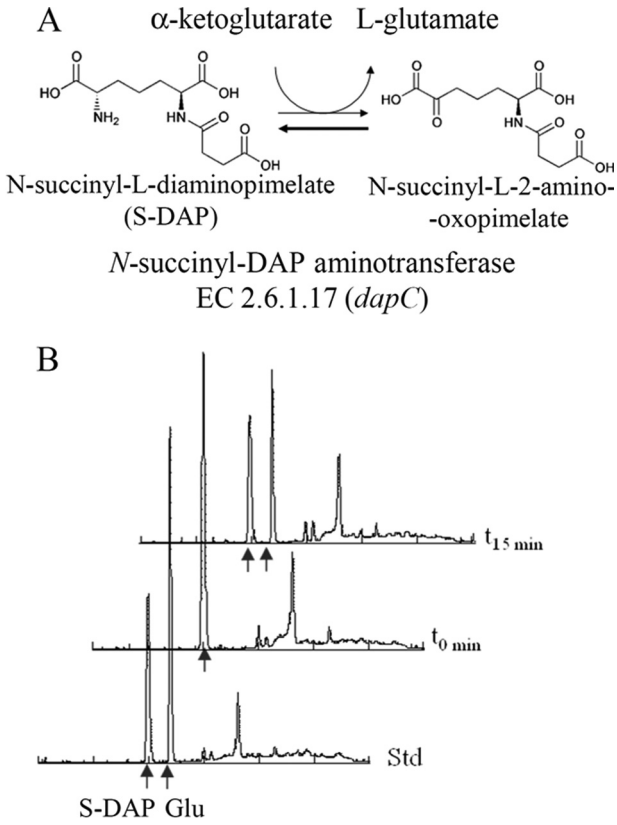

FIGURE 6. **S-DAPAT-catalyzed reaction.** *A*, scheme of the reaction. *B*, HPLC analyses of the reaction. The t_0 reaction mix (100 μl) contained 100 μM S-DAP and 100 μM α-ketoglutarate in 50 mM potassium phosphate buffer (pH 6.9). The reaction was initiated with the recombinant S-DAPAT (Sav_Q82IK5, Mtu_O50434, or Neu_Q82S89). The reactions were allowed to proceed for 15 min at 30 °C and were stopped by centrifugation on Vivaspin 10K concentration units. A 20-μl aliquot of the flow-through was derivatized for 1 min with *o*-phtaldialdehyde prior to its injection on a Spherisorb ODS2 C18 column connected to an Agilent 1100 HPLC system. Elution was carried out at 1 ml/min with a 10–60% methanol gradient (15 min) in 50 mM potassium phosphate buffer (pH 6.9). The *o*-phtaldialdehyde derivatives of amino acids were detected by fluorescence (excitation, 360 nm; emission, 455 nm). Glutamate was identified by comparison with an authentic standard.

PAT Functionalities Were Acquired without Other Modification of Substrate Specificity—We then analyzed the substrate specificity of the three PATs. 1β AAT/PAT (Rme_Q02635), as the previously characterized *Arabidopsis* 1βAAT/PAT *At2g22250* (18, 19), was found highly to be specific toward aspartate and glutamate because it was unable to transfer the amino group of glutamate to phenylpyruvate, 4-hydroxyphenylpyruvate, and 4-methyl-2-oxovalerate. BCAT/PAT (Syn_P54691) was able to transfer the amino group of glutamate to 4-hydroxyphenylpyruvate and phenylpyruvate and unable to transaminate oxaloacetate (Table 3). Its specificity constant (k_{cat}/K_m) for the aromatic substrates phenylpyruvate and 4-hydroxyphenylpyruvate was found to be 10 times smaller than that for prephenate (Table 3). S-DAPAT/PAT (Sav_Q82IK5) was unable to transfer the amino group of glutamate to phenylpyruvate, 4-hydroxyphenylpyruvate, 4-methyl-2-oxovalerate, and oxaloacetate.

PAT Activity Is Not Shared by All 1β AAT, BCAT, or LL-Diaminopimelate Aminotransferase (DAPAT) Enzymes—A possible explanation for the observed PAT diversity could be that all members of these three classes of aminotransferase are able to catalyze prephenate transamination. To address this issue, other 1β AATs, BCATs, and S-DAPATs from *Synechocystis* sp., and *S. avermitilis* were analyzed. We identified by BLAST and cloned two 1β AATs from *Synechocystis* sp. (Syn_Q55128) and from *S. avermitilis* (Sav_Q82DR2), and a BCAT (Sav_Q82JN7) from *S. avermitilis*. All three recombinant aminotransferases were produced in *E. coli* and partially purified (Fig. 7). Because none of them were previously characterized, we first confirmed that they displayed the aminotransferase activities as predicted by their annotation (Table 4). We next analyzed their capacity to transaminate prephenate into arogenate. All three aminotransferases were found to be devoid of detectable PAT activity. We also cloned, expressed in *E. coli*, and partially purified a second annotated S-DAPAT (Sav_Q82EU6) from *S. avermitilis*. However, this aminotransferase appeared to be wrongly annotated because it was found to be unable to transfer the amino group of S-DAP to α-ketoglutarate to yield glutamate. Instead, HPLC analyses revealed that this aminotransferase was able to transfer the amino group of glutamine to α-ketoglutarate (not shown), indicating that this aminotransferase belongs to the closely related family of glutamine transaminase K (EC 3.5.1.2). This enzyme was unable to transaminate prephenate into arogenate using glutamine as amino donor. Finally, the DAPAT (EC 2.6.1.83) of *Synechocystis* (Syn_Q55828) was also analyzed and found to be devoid of PAT activity (cyanobacteria do not harbor any S-DAPAT activity but do possess DAPAT activity (26)).

1β AAT/PAT, BCAT/PAT, and S-DAPAT/PAT Are Observed in Other Proteobacteria, Cyanobacteria, and Actinobacteria—We then investigated whether AAT/PAT could be found in other proteobacteria previously shown to utilize the arogenate

TABLE 3

Substrate specificity of recombinant prephenate aminotransferases

Values given are the average of at least three independent determinations. The difference in each set of data was <10%. All aminotransferases were tested in the presence of 25 mM glutamate and up to a 500 μM concentration of the indicated ketoacids, except for S-DAPAT activity, which was tested in the presence of 5 mM S-DAP and up to 500 μM α-ketoglutarate. 0, no activity detected. OAA: oxaloacetate; 4-MOV: 4-methyl-2-oxovalerate; PP: phenylpyruvate.

	OAA	4-MOV	S-DAP	PP	HPP
AAT/PAT					
Rme_Q02635	$k_{cat} = 205\ s^{-1}$; $K_m = 17\ \mu M$	0	0	0	0
Rsp_A3PMF8	$k_{cat} = 150\ s^{-1}$; $K_m = 27\ \mu M$	0	0	0	0
Neu_Q82WA8	$k_{cat} = 35\ s^{-1}$; $K_m = 33\ \mu M$	0	0	0	0
BCAT/PAT					
Syn_P54691	0	$k_{cat} = 70\ s^{-1}$; $K_m = 45\ \mu M$	0	$k_{cat} = 18\ s^{-1}$; $K_m = 400\ \mu M$	$k_{cat} = 20\ s^{-1}$; $K_m = 450\ \mu M$
Sco_Q3AJX2	0	$k_{cat} = 130\ s^{-1}$; $K_m = 27\ \mu M$	0	0	$k_{cat} = 25\ s^{-1}$; $K_m = 250\ \mu M$
S-DAPAT/PAT					
Sav_Q82IK5	0	0	ND[a]	0	0
Mtu_O50434	0	0	ND	0	0
Neu_Q82S89	0	0	ND	0	0

[a] ND, the capacity of S-DAPAT from *S. avermitilis* (Sav_Q82IK5), *M. tuberculosis* (Mtu_O50434), and *N. europaea* (Neu_Q82S89) to catalyze the transamination of α-ketoglutarate with S-DAP as amino donor was confirmed by spectrophotometry and HPLC (see Fig.6), but the kinetics parameters were not determined.

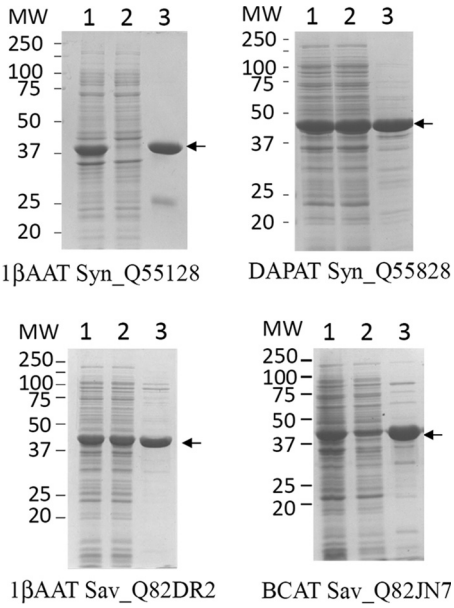

FIGURE 7. **Partial purification of recombinant non-prephenate aminotransferases.** For all proteins, a single Q-Sepharose chromatography step was performed as described under "Experimental Procedures." *Lanes 1*, *2*, and *3* correspond to total extract (20 μg), soluble extract (20 μg), and most active fraction after the purification step (15 μg), respectively.

TABLE 4

Specific activity of recombinant non-prephenate aminotransferases

Activities of the most active fractions eluted from the Q-Sepharose columns (Figs. 7 and 9) were monitored in the presence of saturated concentrations of substrates. OAA, oxaloacetate; 4-MOV, 4-methyl-2-oxovalerate; α-KG, α-ketoglutarate.

AAT	500μM OAA/25mM GLU
Syn_Q55128	19μmol/min /mg
Sav_Q82DR2	45μmol/min /mg
BCAT	500μM 4-MOV/25mM GLU
Sav_Q82JN7	22 μmol/min /mg
Neu_Q82TJ4	60 μmol/min /mg
DAPAT	500μM α-KG/2.5mM S-DAP
Syn_Q55828	4 μmol/min /mg

route (4, 27), BCAT/PAT in another cyanobacterium, and S-DAPAT/PAT in another actinobacterium. BLAST searches with the three previously identified PAT sequences allowed the identification of putative orthologs in a second bacterium in each class. The highest score returned by the BLAST searches were for 1β AAT (Rsp_A3PMF8) and 1β AAT (Neu_Q82WA8) in the α-proteobacterium *R. sphaeroides* and the β-proteobacterium *N. europaea*, respectively, a BCAT (Sco_Q3AJX2) in the cyanobacterium *Synechococcus* sp., and an S-DAPAT (Mtu_O50434) in the actinobacterium *M. tuberculosis*. The genes of these four aminotransferases were cloned, and the corresponding proteins were overproduced in *E. coli* and characterized. As shown in Table 2 and Fig. 8, all orthologs effectively displayed *bona fide* PAT activity in addition to the expected aminotransferase activities. With the exception of the 1β AAT (Neu_Q82WA8) from *N. europaea*, the kinetic parameters of these proteins for the transamination of prephenate were of the same order of magnitude as those of their orthologs first characterized (Table 2). They all present the same substrate specificity as their respective orthologs (Table 3). The PAT specificity (k_{cat}/K_m) of 1β AAT (Neu_Q82WA8) was found to be 50–1000 times lower than that of the corresponding 1β AAT orthologs Rsp_A3PMF8 and Rme_Q02635 (k_{cat}/K_m was 0.002 $\mu M^{-1} \cdot s^{-1}$ compared with 0.08–2.6 $\mu M^{-1} \cdot s^{-1}$ for the other PATs characterized).

N. europaea Possesses Two Distinct PAT Activities—N. europaea is known to exclusively use the arogenate route for tyrosine biosynthesis (9); however, although measurable, the PAT activity displayed by Neu_Q82WA8 appears too low to be of physiological relevance. We thus checked whether PAT activity could be sustained by another aminotransferase (AAT, BCAT, or S-DAPAT) in *N. europaea*. BLAST searches with the previously identified AAT/PAT, BCAT/PAT, and S-DAPAT/PAT sequences allowed the identification of putative orthologs: two BCATs (Neu_Q82TJ4 and Neu_Q82UJ8) and a S-DAPAT (Neu_Q82S89). No 1β AAT ortholog could be identified. The genes of these three aminotransferases were cloned, and the corresponding proteins were overproduced in *E. coli* and partially purified (Fig. 9). The corresponding recombinant proteins were characterized, and with the exception of the predicted BCAT ortholog (Neu_Q82UJ8), which was found in this study to be a D-alanine aminotransferase (EC 2.6.1.21), the remaining two orthologs displayed the aminotransferase activities expected from their annotations (Table 4 and Fig. 6). The analyses of their respective capacity to catalyze PAT activity

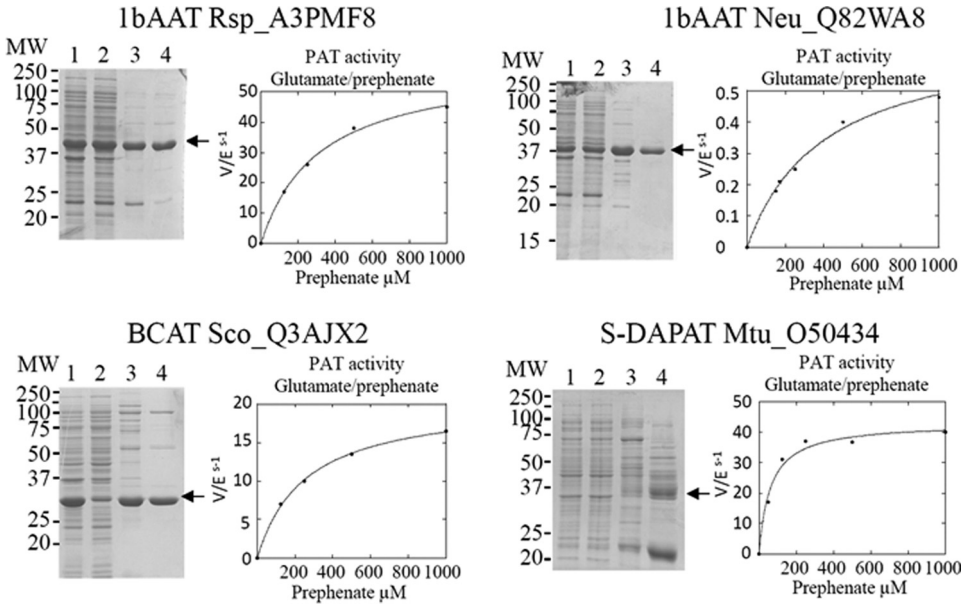

FIGURE 8. **Partial purification of recombinant prephenate aminotransferase hortologs and kinetic analyses of their respective PAT activities.** The curves are the best fits obtained by non-linear regression analyses of the data points using the equation for a hyperbola. *MW*, molecular weight. *Lane 1*, total extract (20 μg); *lane 2*, soluble extract (20 μg); *lane 3*, pool of the fractions containing PAT activity eluted from the EMD-DEAE column (10 μg); *lane 4*, most active fraction eluted from the Superdex S200 column (10 μg).

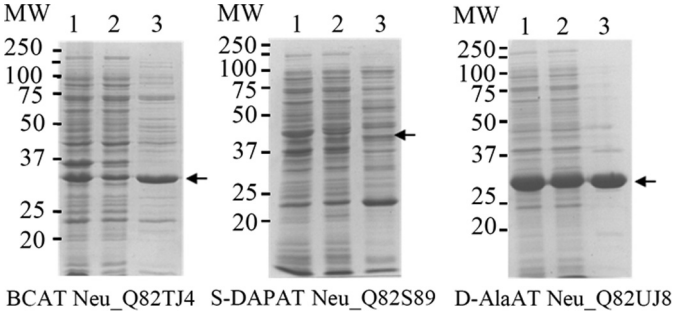

FIGURE 9. **Partial purification of recombinant *N. europea* aminotransferases.** For all proteins, a single Q-Sepharose chromatography was performed as described under "Experimental Procedures." *Lanes 1–3* correspond to total extract (20 μg), soluble extract (20 μg), and the most active fractions eluted from the Q-Sepharose column (15 μg), respectively.

revealed that the S-DAPAT Neu_Q82S89 displayed *bona fide* PAT activity that compared well with the PAT activity of the S-DAPAT/PAT Sav_Q82IK5 and Mtu_O50434, both in terms of activity and substrate specificity (Tables 2 and 3). The other two aminotransferases were found to be devoid of any detectable PAT activity. *N. europaea* thus possesses a second PAT much more efficient than the previously found 1β AAT Neu_Q82WA8.

DISCUSSION

In the present study, we analyzed the arogenate route alternative in the synthesis of the aromatic amino acid tyrosine in three different arogenate-competent prokaryote phyla (proteobacteria, cyanobacteria, and actinobacteria) through the identification of PAT functionality in seven bacterial strains. Our results revealed that the nature of the aminotransferase conferring PAT activity differs depending on the tested microorganisms. PAT activity is housed by a 1β AAT in the α-proteobacteria *R. meliloti* and *R. sphaeroides* and the β-proteobacterium *N. europaea*, by a BCAT in the cyanobacteria *Synechocystis* sp. and *Synechococcus* sp., and by an S-DAPAT in the actinobacteria *S. avermitilis* and *M. tuberculosis* and the β-proteobacterium *N. europaea*.

The variety and the identity of PAT enzymes could not be anticipated from previous biochemical analyses of arogenate-dependent organisms, but puzzling previous observations can now be explained in the light of our results. In the first report of arogenate synthesis in the cyanobacterium *Agmenellum quadruplicatum* (4, 27), leucine, isoleucine, and phenylalanine proved to be efficient amino-donors. This is now explained by our identification of BCAT/PATs in *Synechocystis* and *Synechococcus*, which both effectively present some aromatic aminotransferase activity (Table 3) in addition to their BCAT and PAT activity. Also, the observation (28) that in the actinobacterium *Amycolatopsis methanolica* none of the tested amino-donors, except glutamate, allowed detection of prephenate aminotransferase activity can be explained by the identification of a totally unexpected PAT housed by a highly specific S-DAPAT in the two actinobacteria analyzed.

The three classes of aminotransferase presently found to support arogenate synthesis belong to two different fold types of PLP-dependent enzymes. 1β AAT and S-DAPAT are structurally related because they both belong to the fold type I. By contrast, BCATs belong to the fold type IV, which is structurally unrelated to fold type I (29). This reveals that PAT function could not originate from a common aminotransferase ancestor because the two fold types are evolutionarily distinct (29, 30) and suggests that the arogenate route has arisen more than once during evolution. The acquisition of PAT functionality by three different aminotransferases reflects the plasticity of these enzymes. Interestingly, our results reveal that these aminotransferases have gained PAT functionalities without any noticeable change in their original substrate specificity (Table 3).

From an evolutionary point of view, the *N. europaea* case is interesting because this organism harbors two different PATs, a 1β AAT/PAT, as observed in the closely related α-proteobacteria, and an S-DAPAT/PAT, as found in the more distantly related actinobacteria. Two scenarios may explain this observation; either *N. europaea* has acquired its S-DAPAT/PAT by horizontal gene transfer from an actinobacterium, or it has independently evolved it from an endogenous S-DAPAT. A phylogenetic analysis might help argue in favor of one or the other possibility. However, this is not yet possible due to the low number of S-DAPATs characterized to date (three in this study and only two others previously studied: one in the β-proteobacterium *Bordetella pertussis* (31) and another one in the actinobacteria *Corynebacterium glutamicum* (32)).

Our present finding that PAT functionality has distinct origins also suggests that although plant aromatic amino acids are exclusively synthesized in the chloroplast (33), the plant arogenate route did not originate from cyanobacteria, which possess a BCAT/PAT. Most probably, the 1β AAT/PAT encoded by the *At2g22250* gene was acquired either via the mitochondrial ancestor or via a lateral gene transfer event.

The evolution of a new functionality in different classes of aminotransferases has been previously described for the conversion of ketomethiobutyrate into methionine in the last step of the methionine regeneration pathway. In some microorganisms, a broad specific aspartate aminotransferase was found to be the enzyme responsible; in others, it was a broad specific tyrosine aminotransferase; and in Gram-positive bacteria, it was a BCAT (34). PAT activity thus appears to be another example of this capacity of aminotransferases from different PLP fold types to evolve convergent functionality; however, PAT functionalities were gained by aminotransferases with high substrate specificities.

In contrast to the methionine regeneration pathway that is present in all organisms, the arogenate route is found only in some organisms. We can thus take advantage of this feature to tentatively search for the evolutionary benefit provided by the arogenate alternative. A metabolic consequence of tyrosine synthesis from arogenate is the exclusion of 4-hydroxyphenylpyruvate (4-HPP) as an intermediate in the tyrosine biosynthesis pathway (Fig. 10). Interestingly, this exclusion could avoid futile cycling in microorganisms containing the tyrosine catabolic pathway, which proceeds via 4-HPP and then homogentisate. Microorganisms devoid of this catabolic pathway, which involves the presence of 4-hydroxyphenylpyruvate dioxygenase (4-HPPD) and of 1,2-homogentisate dioxygenase (1,2-HGAD) (35, 36) and leads ultimately to fumarate and acetoacetate, are unable to grow on tyrosine as a single carbon and nitrogen source (37). We thus checked using BLAST searches in the NCBI genomic database for a possible association between the presence of the arogenate route and the presence of the tyrosine catabolic pathway. We observed the following. (i) 4-HPPD and 1,2-HGAD orthologs are found in the majority of α-proteobacteria, most β-proteobacteria, and most actinobacteria, two bacterial classes and one bacterial phylum reported to synthesize tyrosine via the arogenate route (38) (this work). (ii) 4-HPPD and 1,2-HGAD are absent in the Gram-positive *Bacillus*

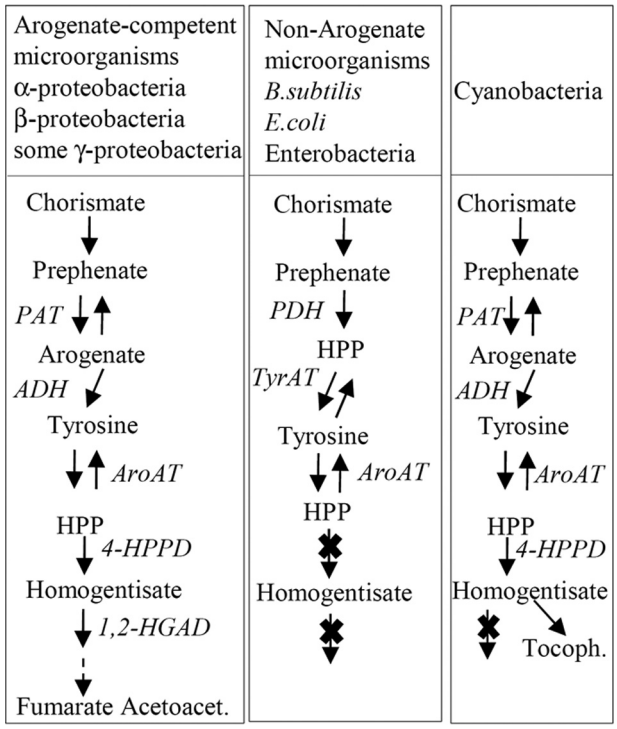

FIGURE 10. **Different organizations of tyrosine metabolism in prokaryotes.** *ADH*, arogenate dehydrogenase; *ADT*, arogenate dehydratase; *AroAT*, aromatic aminotransferase; *E4P*, erythrose 4-phosphate; *PAT*, prephenate aminotransferase; *PDH*, prephenate dehydrogenase; *PEP*, phosphoenolpyruvate; *Tyr-AT*, tyrosine aminotransferase; *HPP*, 4-hydroxyphenylpyruvate; *HGA*, homogentisate; *4-HPPD*, 4-hydroxyphenylpyruvate dioxygenase; *1,2-HGAD*, 1,2-homogentisate dioxygenase; *Acetoacet*., acetoacetate; *Tocoph*., tocopherols.

subtilis, a microorganism proven to synthesize tyrosine via 4-HPP (39) and thus lacking the arogenate route. (iii) BLAST analyses also revealed the absence of 4-HPPD and 1,2-HGAD in all enterobacteria that have been proven (*E. coli* (40, 41)) or predicted (38, 42) to synthesize tyrosine via 4-HPP by a fusion between chorismate mutase (AroQ) and prephenate dehydrogenase (TYRA) (38, 42); (iv) BLAST analyses also revealed that in cyanobacteria, the presence of the arogenate route is linked to the presence of 4-HPPD but not of 1,2-HGAD. In these photosynthetic microorganisms, as in plants (43), homogentisate provided by 4-HPPD is the aromatic precursor of vitamins E. The presence of tyrosine degradation enzymes in arogenate-competent microorganisms and their absence in arogenate-incompetent microorganisms suggest that one possible driving force behind the convergent emergence and fixation during evolution of the arogenate route was the exclusion of 4-HPP from the tyrosine biosynthetic pathway (Fig. 10). This exclusion certainly provided a selective advantage for prokaryotes evolving a tyrosine catabolic route via 4-HPP and homogentisate or using homogentisate as a starting block for new metabolites.

Finally, besides identifying three distinct origins of PAT functionality and illuminating possible drivers for the evolution of metabolic pathways for the aromatic amino acids, our results provide the identification of 15 aminotransferases. One, the S-DAPAT/PAT from *M. tuberculosis* Mtu_O50434, presents pharmacological interest as an antibacterial drug target.

Acknowledgments—We thank James Connorton for the English correction of the manuscript and Elisa Dell'Aglio for help during the review process; Dr. Mengin-Lecreulx for the gift of N-succinyl-LL-diaminopimelate; G. Alloing (Sophia Antipolis, France) for providing the R. meliloti RCR2011 strain; G. Ajlani (Saclay, France) for providing Synechocystis sp. PCC 6803; and M. Sabaty (Institut Pasteur, Paris, France) for providing the S. avermitilis strain.

REFERENCES

1. Haslam, E. (1993) *Shikimic Acid, Metabolism and Metabolites*, Wiley, Chichester, UK
2. Razal, R. A., Ellis, S., Singh, S., Lewis, N. G., and Towers, G. H. N. (1996) Nitrogen recycling in phenylpropanoid metabolism. *Phytochemistry* **41,** 31–35
3. Dewick, P. M. (1998) The biosynthesis of shikimate metabolites. *Nat. Prod. Rep.* **15,** 17–58
4. Stenmark, S. L., Pierson, D. L., and Jensen, R. A. (1974) Blue-green bacteria synthesize L-tyrosine by pretyrosine pathway. *Nature* **247,** 290–292
5. Hall, G. C., Flick, M. B., Gherna, R. L., and Jensen, R. A. (1982) Biochemical diversity for biosynthesis of aromatic-amino-acids among the Cyanobacteria. *J. Bacteriol.* **149,** 65–78
6. Fazel, A. M., and Jensen, R. A. (1979) Obligatory biosynthesis of L-tyrosine via the pretyrosine branchlet in coryneform bacteria. *J. Bacteriol.* **138,** 805–815
7. Christendat, D., and Turnbull, J. L. (1999) Identifying groups involved in the binding of prephenate to prephenate dehydrogenase from *Escherichia coli*. *Biochemistry* **38,** 4782–4793
8. Patel, N., Pierson, D. L., and Jensen, R. A. (1977) Dual enzymatic routes to L-tyrosine and L-phenylalanine via pretyrosine in *Pseudomonas aeruginosa*. *J. Biol. Chem.* **252,** 5839–5846
9. Zhao, G., Xia, T., Ingram, L. O., and Jensen, R. A. (1993) An allosterically insensitive class of cyclohexadienyl dehydrogenase from *Zymomonas mobilis*. *Eur. J. Biochem.* **212,** 157–165
10. Jung, E., Zamir, L. O., and Jensen, R. A. (1986) Chloroplasts of higher-plants synthesize L-phenylalanine via L-arogenate. *Proc. Natl. Acad. Sci. U.S.A.* **83,** 7231–7235
11. Rippert, P., and Matringe, M. (2002) Molecular and biochemical characterization of an *Arabidopsis thaliana* arogenate dehydrogenase with two highly similar and active protein domains. *Plant Mol. Biol.* **48,** 361–368
12. Rippert, P., and Matringe, M. (2002) Purification and kinetic analysis of the two recombinant arogenate dehydrogenase isoforms of *Arabidopsis thaliana*. *Eur. J. Biochem.* **269,** 4753–4761
13. Cho, M. H., Corea, O. R., Yang, H., Bedgar, D. L., Laskar, D. D., Anterola, A. M., Moog-Anterola, F. A., Hood, R. L., Kohalmi, S. E., Bernards, M. A., Kang, C., Davin, L. B., and Lewis, N. G. (2007) Phenylalanine biosynthesis in *Arabidopsis thaliana*. Identification and characterization of arogenate dehydratases. *J. Biol. Chem.* **282,** 30827–30835
14. Byng, G., Whitaker, R., Flick, C., and Jensen, R. A. (1981) Enzymology of L-tyrosine biosynthesis in corn (*Zea mays*). *Phytochemistry* **20,** 1289–1292
15. Connelly, J. A., and Conn, E. E. (1986) Tyrosine biosynthesis in *Sorghum bicolor*. Isolation and regulatory properties of arogenate dehydrogenase. *Z. Naturforsch.* **41,** 69–78
16. Siehl, D. L., Connelly, J. A., and Conn, E. E. (1986) Tyrosine biosynthesis in *Sorghum bicolor*. Characteristics of prephenate aminotransferase. *Z. Naturforsch.* **41,** 79–86
17. Siehl, D. L., and Conn, E. E. (1988) Kinetic and regulatory properties of arogenate dehydratase in seedlings of *Sorghum bicolor* (l.) *moench*. *Arch. Biochem. Biophys.* **260,** 822–829
18. Graindorge, M., Giustini, C., Jacomin, A. C., Kraut, A., Curien, G., and Matringe, M. (2010) Identification of a plant gene encoding glutamate/aspartate-prephenate aminotransferase. The last homeless enzyme of aromatic amino acids biosynthesis. *FEBS Lett.* **584,** 4357–4360
19. Maeda, H., Yoo, H., and Dudareva, N. (2011) Prephenate aminotransferase directs plant phenylalanine biosynthesis via arogenate. *Nat. Chem. Biol* **7,** 19–21
20. Jensen, R. A., and Gu, W. (1996) Evolutionary recruitment of biochemically specialized subdivisions of family I within the protein superfamily of aminotransferases. *J. Bacteriol.* **178,** 2161–2171
21. Subramaniam, P., Bhatnagar, R., Hooper, A., and Jensen, R. A. (1994) The dynamic progression of evolved character states for aromatic amino-acid biosynthesis in Gram-negative bacteria. *Microbiology* **140,** 3431–3440
22. Kraut, A., Marcellin, M., Adrait, A., Kuhn, L., Louwagie, M., Kieffer-Jaquinod, S., Lebert, D., Masselon, C. D., Dupuis, A., Bruley, C., Jaquinod, M., Garin, J., and Gallagher-Gambarelli, M. (2009) Peptide storage. Are you getting the best return on your investment? Defining optimal storage conditions for proteomics samples. *J Proteome Res.* **8,** 3778–3785
23. Bernay, B., Gaillard, M. C., Guryca, V., Emadali, A., Kuhn, L., Bertrand, A., Detraz, I., Carcenac, C., Savasta, M., Brouillet, E., Garin, J., and Elalouf, J. M. (2009) Discovering new bioactive neuropeptides in the striatum secretome using *in vivo* microdialysis and versatile proteomics. *Mol. Cell Proteomics* **8,** 946–958
24. Legrand, P., Dumas, R., Seux, M., Rippert, P., Ravelli, R., Ferrer, J. L., and Matringe, M. (2006) Biochemical characterization and crystal structure of *Synechocystis* arogenate dehydrogenase provide insights into catalytic reaction. *Structure* **14,** 767–776
25. Scapin, G., and Blanchard, J. S. (1998) Enzymology of bacterial lysine biosynthesis. *Adv. Enzymol. Relat. Areas Mol. Biol.* **72,** 279–324
26. Hudson, A. O., Singh, B. K., Leustek, T., and Gilvarg, C. (2006) An LL-diaminopimelate aminotransferase defines a novel variant of the lysine biosynthesis pathway in plants. *Plant Physiol.* **140,** 292–301
27. Jensen, R. A., and Pierson, D. L. (1975) Evolutionary implications of different types of microbial enzymology for L-tyrosine biosynthesis. *Nature* **254,** 667–671
28. Abou-Zeid, A., Euverink, G., Hessels, G. I., Jensen, R. A., and Dijkhuizen, L. (1995) Biosynthesis of L-phenylalanine and L-tyrosine in the actinomycete *Amycolatopsis methanolica*. *Appl. Environ. Microbiol.* **61,** 1298–1302
29. Mehta, P. K., and Christen, P. (2000) The molecular evolution of pyridoxal-5′-phosphate-dependent enzymes. *Adv. Enzymol.* **74,** 129–184
30. Eliot, A. C., and Kirsch, J. F. (2004) Pyridoxal phosphate enzymes. Mechanistic, structural, and evolutionary considerations. *Annu. Rev. Biochem.* **73,** 383–415
31. Fuchs, T. M., Schneider, B., Krumbach, K., Eggeling, L., and Gross, R. (2000) Characterization of a *Bordetella pertussis* diaminopimelate (DAP) biosynthesis locus identifies *dapC*, a novel gene coding for an *N*-succinyl-L,L-DAP aminotransferase. *J. Bacteriol.* **182,** 3626–3631
32. Hartmann, M., Tauch, A., Eggeling, L., Bathe, B., Möckel, B., Pühler, A., and Kalinowski, J. (2003) Identification and characterization of the last two unknown genes, *dapC* and *dapF*, in the succinylase branch of the L-lysine biosynthesis of *Corynebacterium glutamicum*. *J. Biotechnol.* **104,** 199–211
33. Rippert, P., Puyaubert, J., Grisollet, D., Derrier, L., and Matringe, M. (2009) Tyrosine and phenylalanine are synthesized within the plastids in *Arabidopsis*. *Plant Physiol.* **149,** 1251–1260
34. Berger, B. J., English, S., Chan, G., and Knodel, M. H. (2003) Methionine regeneration and aminotransferases in *Bacillus subtilis*, *Bacillus cereus*, and *Bacillus anthracis*. *J. Bacteriol.* **185,** 2418–2431
35. Lindstedt, S., Odelhög, B., and Rundgren, M. (1977) Purification and some properties of 4-hydroxyphenylpyruvate dioxygenase from pseudomona SP P.J. 874. *Biochemistry* **16,** 3369–3377
36. Arias-Barrau, E., Olivera, E. R., Luengo, J. M., Fernández, C., Galán, B., García, J. L., Díaz, E., and Miñambres, B. (2004) The homogentisate pathway. A central catabolic pathway involved in the degradation of L-phenylalanine, L-tyrosine, and 3-hydroxyphenylacetate in *Pseudomonas putida*. *J. Bacteriol.* **186,** 5062–5077
37. Large, P. J. (1986) Degradation of organic nitrogen compounds by yeasts. *Yeast* **2,** 1–34
38. Bonner, C. A., Disz, T., Hwang, K., Song, J., Vonstein, V., Overbeek, R., and Jensen, R. A. (2008) Cohesion group approach for evolutionary analysis of TyrA, a protein family with wide-ranging substrate Specificities. *Microbiol. Mol. Biol. Rev.* **72,** 13–53, table of contents
39. Champney, W. S., and Jensen, R. A. (1970) Enzymology of prephenate

dehydrogenase in *Bacillus subtilis*. *J. Biol. Chem.* **245,** 3763–3770
40. Koch, G. L., Shaw, D. C., and Gibson, F. (1971) Purification and characterisation of chorismate mutase-prephenate dehydrogenase from *Escherichia coli*-K12. *Biochim. Biophys. Acta* **229,** 795–804
41. Turnbull, J., and Morrison, J. F. (1990) Chorismate mutase prephenate dehydrogenase from *Escherichia coli.* 2. Evidence for 2 different active-sites. *Biochemistry* **29,** 10255–10261
42. Song, J., Bonner, C. A., Wolinsky, M., and Jensen, R. A. (2005) The TyrA family of aromatic-pathway dehydrogenases in phylogenetic context. *BMC Biol.* **3,** 13
43. Garcia, I., Rodgers, M., Lenne, C., Rolland, A., Sailland, A., and Matringe, M. (1997) Subcellular localization and purification of a *p*-hydroxyphenylpyruvate dioxygenase from cultured carrot cells and characterization of the corresponding cDNA. *Biochem. J.* **325,** 761–769